

# VDT: GENERAL-PURPOSE VIDEO DIFFUSION TRANSFORMERS VIA MASK MODELING

Haoyu Lu<sup>1</sup> Guoxing Yang<sup>1</sup> Nanyi Fei<sup>1</sup> Yuqi Huo<sup>4</sup> Zhiwu Lu<sup>1,\*</sup> Ping Luo<sup>3</sup> Mingyu Ding<sup>2,\*</sup>

<sup>1</sup>Gaoling School of Artificial Intelligence, Renmin University of China, Beijing, China

<sup>2</sup>University of California, Berkeley, United States

<sup>3</sup>The University of Hong Kong, Pokfulam, Hong Kong

<sup>4</sup>Baichuan Inc.

{lhy1998, luzhiwu}@ruc.edu.cn

myding@berkeley.edu

## ABSTRACT

This work introduces Video Diffusion Transformer (VDT), which pioneers the use of transformers in diffusion-based video generation. It features transformer blocks with modularized temporal and spatial attention modules to leverage the rich spatial-temporal representation inherited in transformers. Additionally, we propose a unified spatial-temporal mask modeling mechanism, seamlessly integrated with the model, to cater to diverse video generation scenarios.

VDT offers several appealing benefits. **1)** It excels at capturing temporal dependencies to produce temporally consistent video frames and even simulate the physics and dynamics of 3D objects over time. **2)** It facilitates flexible conditioning information, *e.g.*, simple concatenation in the token space, effectively unifying different token lengths and modalities. **3)** Pairing with our proposed spatial-temporal mask modeling mechanism, it becomes a general-purpose video diffuser for harnessing a range of tasks, including unconditional generation, video prediction, interpolation, animation, and completion, etc. Extensive experiments on these tasks spanning various scenarios, including autonomous driving, natural weather, human action, and physics-based simulation, demonstrate the effectiveness of VDT. Additionally, we present comprehensive studies on how VDT handles conditioning information with the mask modeling mechanism, which we believe will benefit future research and advance the field. Codes and models are available at [VDT-2023.github.io](https://github.com/VDT-2023).

## 1 INTRODUCTION

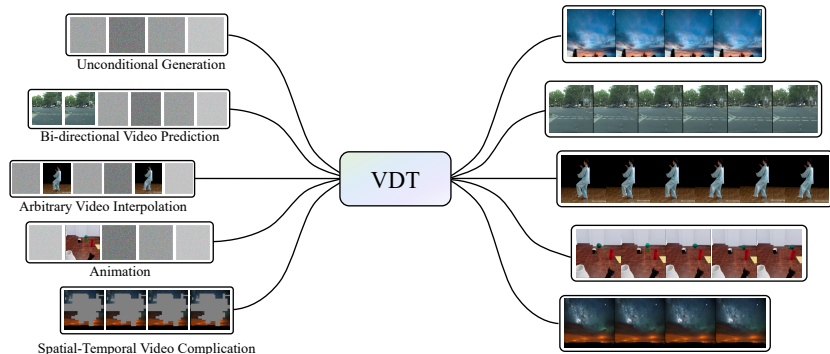


Figure 1: A diagram of our unified video diffusion transformer (VDT) via spatial-temporal mask modeling. VDT represents a versatile framework constructed upon pure transformer architectures.

Recent years have witnessed significant achievements in artificial intelligence generated content (AIGC), where diffusion models have emerged as a central technique being extensively studied in image (Nichol & Dhariwal, 2021; Dhariwal & Nichol, 2021) and audio domains (Kong et al.,

\*Corresponding authors.

2020; Huang et al., 2023). For example, methods like DALL-E 2 (Ramesh et al., 2022) and Stable Diffusion (Rombach et al., 2022) can generate high-quality images given textual description. However, diffusion approaches in the video domain, while attracting a lot of attention, still lag behind. The challenges lie in effectively modeling temporal information to generate temporally consistent high-quality video frames, and unifying a variety of video generation tasks including unconditional generation, prediction, interpolation, animation, and completion, as shown in Figure 1.

Recent works (Voleti et al., 2022; Ho et al., 2022b;a; Yang et al., 2022; He et al., 2022; Wu et al., 2022a; Esser et al., 2023; Yu et al., 2023b; Wang et al., 2023b) have introduced video generation and prediction methods based on diffusion techniques, where U-Net (Ronneberger et al., 2015) is commonly adopted as the backbone architecture. Few studies have shed light on diffusion approaches in the video domain with alternative architectures. Considering the exceptional success of the transformer architecture across diverse deep learning domains and its inherent capability to handle temporal data, we raise a question: *Is it feasible to employ vision transformers as the backbone model in video diffusion?* Transformers have been explored in the domain of image generation, such as DiT (Peebles & Xie, 2022) and U-ViT (Bao et al., 2022), showcasing promising results. When applying transformers to video diffusion, several unique considerations arise due to the temporal nature of videos.

Transformers offer several advantages in the video domain. **1)** The domain of video generation encompasses a variety of tasks, such as unconditional generation, video prediction, interpolation, and text-to-image generation. Prior research (Voleti et al., 2022; He et al., 2022; Yu et al., 2023b; Blattmann et al., 2023) has typically focused on individual tasks, often incorporating specialized modules for downstream fine-tuning. Moreover, these tasks involve diverse conditioning information that can vary across frames and modalities. This necessitates a robust architecture capable of handling varying input lengths and modalities. The integration of transformers can facilitate the seamless unification of these diverse tasks. **2)** Transformers, unlike U-Net which is designed mainly for images, are inherently capable of capturing long-range or irregular temporal dependencies, thanks to their powerful tokenization and attention mechanisms. This enables them to better handle the temporal dimension, as evidenced by superior performance compared to convolutional networks in various video tasks, including classification (Wang et al., 2022b; 2023a), localization (Zhang et al., 2022; Wang et al., 2023a), and retrieval (Wang et al., 2022a; Lu et al., 2022). **3)** Only when a model has learned (or memorized) worldly knowledge (e.g., spatiotemporal relationships and physical laws) can it generate videos corresponding to the real world. Model capacity is thus a crucial component for video diffusion. Transformers have proven to be highly scalable, making them more suitable than 3D-U-Net (Ho et al., 2022b; Blattmann et al., 2023; Wang et al., 2023c) for tackling the challenges of video generation. For example, the largest U-Net, SD-XL (Podell et al., 2023), has 2.6B parameters, whereas transformers, like PaLM (Narang & Chowdhery, 2022), boast 540B.

Inspired by the above analysis, this study presents a thorough exploration of applying transformers to video diffusion and addresses the unique challenges it poses, such as the accurate capturing of temporal dependencies, the appropriate handling of conditioning information, and unifying diverse video generation tasks. Specifically, we propose Video Diffusion Transformer (VDT) for video generation, which comprises transformer blocks equipped with temporal and spatial attention modules, a VAE tokenizer for effective tokenization, and a decoder to generate video frames. VDT offers several appealing benefits. **1)** It excels at capturing temporal dependencies, including both the evolution of frames and the dynamics of objects over time. The powerful temporal attention module also ensures the generation of high-quality and temporally consistent video frames. **2)** Benefiting from the flexibility and tokenization capabilities of transformers, conditioning the observed video frames is straightforward. For example, a simple token concatenation is sufficient to achieve remarkable performance. **3)** The design of VDT is paired with a unified spatial-temporal mask modeling mechanism, harnessing diverse video generation tasks (see Figure 1), e.g., unconditional video generation, bidirectional video forecasting, arbitrary video interpolation, and dynamic video animation. Our proposed training mechanism positions VDT as a general-purpose video diffuser.

Our contributions are three-fold.

- We pioneer the utilization of transformers in diffusion-based video generation by introducing our Video Diffusion Transformer (VDT). To the best of our knowledge, this marks the first successful model in transformer-based video diffusion, showcasing the potential in this domain.

- We introduce a unified spatial-temporal mask modeling mechanism for VDT, combined with its inherent spatial-temporal modeling capabilities, enabling it to unify a diverse array of general-purpose tasks with state-of-the-art performance, including capturing the dynamics of 3D objects on the physics-QA dataset (Bear et al., 2021).
- We present a comprehensive study on how VDT can capture accurate temporal dependencies, handle conditioning information, and be efficiently trained, etc. By exploring these aspects, we contribute to a deeper understanding of transformer-based video diffusion and advance the field.

## 2 RELATED WORK

**Diffusion Model.** Recently, diffusion models (Sohl-Dickstein et al., 2015; Song & Ermon, 2019; Ho et al., 2020; Choi et al., 2021) have shown great success in the generation field. (Ho et al., 2020) firstly introduced a noise prediction formulation for image generation, which generates images from pure Gaussian noises by denoising noise step by step. Based on such formulation, numerous improvements have been proposed, which mainly focus on sample quality (Rombach et al., 2021), sampling efficiency (Song et al., 2021), and condition generation (Ho & Salimans, 2022). Besides image generation, diffusion models have also been applied to various domains, including audio generation (Kong et al., 2020; Huang et al., 2023), video generation (Ho et al., 2022b), and point cloud generation (Luo & Hu, 2021). Although most of the previous works adopt U-Net based architectures in diffusion model, transformer-based diffusion model has been recently proposed by (Peebles & Xie, 2022; Bao et al., 2022) for image generation, which can achieve comparable results with U-Net based architecture in image generation. In this paper, due to the superior temporal modeling ability of transformer, we explore the use of the transformer-based diffusion model for video generation and prediction.

**Video Generation and Prediction.** Video generation and video prediction are two highly challenging tasks that has gained significant attention in recent years due to the explosive growth of web videos. Previous works (Vondrick et al., 2016; Saito et al., 2017) have adopted GANs to directly learn the joint distribution of video frames, while others (Esser et al., 2021; Ge et al., 2022; Gupta et al., 2023; Yu et al., 2023a) have adopted a vector quantized autoencoder followed by a transformer to learn the distribution in the quantized latent space. For video generation, several poisoners works (Ho et al., 2022b; He et al., 2022; Blattmann et al., 2023; Wang et al., 2023c; Yu et al., 2023b; Wang et al., 2023b) extend the 2D U-Net by incorporating temporal attention into 2D convolution kernels to learn both temporal and spatial features simultaneously. Diffusion has been employed for video prediction tasks in recent works (Voleti et al., 2022; Yang et al., 2022), which utilize specialized modules to incorporate the 2D U-Net network and generate frames based on previously generated frames. Prior research has primarily centered on either video generation or prediction, rarely excelling at both simultaneously. In this paper, we present VDT, a video diffusion model rooted in a pure transformer architecture. Our VDT showcases strong video generation potential and can seamlessly extend to and perform well on a broader array of video generation tasks through our unified spatial-temporal mask modeling mechanism, without requiring modifications to the underlying architecture.

## 3 METHOD

We introduce the Video Diffusion Transformer (VDT) as a unified framework for diffusion-based video generation. We present an overview in Section 3.1, and then delve into the details of applying our VDT to the conditional video generation in Section 3.2. In Section 3.3, we show how VDT be extended for a diverse array of general-purpose tasks via unified spatial-temporal mask modeling.

### 3.1 OVERALL FRAMEWORK

In this paper, we focus on exploring the use of transformer-based diffusion in video generation, and thus adopt the traditional transformer structure for video generation and have not made significant modifications to it. The influence of the transformer architecture in video generation is left to future work. The overall architecture of our proposed video diffusion transformer (VDT) is presented in Fig 2. VDT parameterizes the noise prediction network.

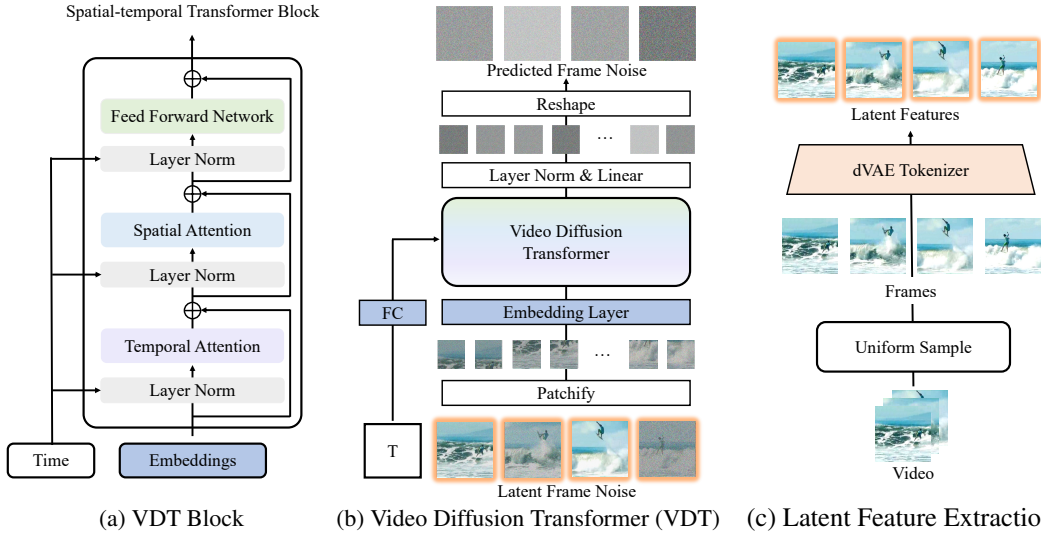


Figure 2: Illustration of our video diffusion transformer (VDT). (a) VDT block with temporal and spatial attention. (b) The diffusion pipeline of our VDT. (c) We uniformly sample frames and then project them into the latent space using a pre-trained VAE tokenizer.

**Input/Output Feature.** The objective of VDT is to generate a video clip  $\in R^{F \times H \times W \times 3}$ , consisting of  $F$  frames of size  $H \times W$ . However, using raw pixels as input for VDT can lead to extremely heavy computation, particularly when  $F$  is large. To address this issue, we take inspiration from the LDM (Rombach et al., 2022) and project the video into a latent space using a pre-trained VAE tokenizer from LDM. This speeds up our VDT by reducing the input and output to latent feature/noise  $\mathcal{F} \in R^{F \times H/8 \times W/8 \times C}$ , consisting of  $F$  frame latent features of size  $H/8 \times W/8$ . Here, 8 is the downsample rate of the VAE tokenizer, and  $C$  denotes the latent feature dimension.

**Linear Embedding.** Following the approach of Vision Transformer (ViT) (Dosovitskiy et al., 2021), we divide the latent feature representation into non-overlapping patches of size  $N \times N$  in the spatial dimension. In order to explicitly learn both spatial and temporal information, we add spatial and temporal positional embeddings (sin-cos) to each patch.

**Spatial-temporal Transformer Block.** Inspired by the success of space-time self-attention in video modeling, we insert a temporal attention layer into the transformer block to obtain the temporal modeling ability. Specifically, each transformer block consists of a multi-head temporal-attention, a multi-head spatial-attention, and a fully connected feed-forward network, as shown in Figure 2.

During the diffusion process, it is essential to incorporate time information into the transformer block. Following the adaptive group normalization used in U-Net based diffusion model, we integrate the time component after the layer normalization in the transformer block, which can be formulated as:

$$adaLN(h, t) = t_{scale} LayerNorm(h) + t_{shift}, \tag{1}$$

where  $h$  is the hidden state and  $t_{scale}$  and  $t_{shift}$  are scale and shift parameters obtained from the time embedding.

### 3.2 CONDITIONAL VIDEO GENERATION SCHEME FOR VIDEO PREDICTION

In this section, we explore how to extend our VDT model to video prediction, or in other words, conditional video generation, where given/observed frames are conditional frames.

**Adaptive layer normalization.** A straightforward approach to achieving video prediction is to incorporate conditional frame features into the layer normalization of transformer block, similar to how we integrate time information into the diffusion process. The Eq 1 can be formulated as:

$$adaLN(h, c) = c_{scale} LayerNorm(h) + c_{shift}, \tag{2}$$

where  $h$  is the hidden state and  $c_{scale}$  and  $c_{shift}$  are scale and shift parameters obtained from the time embedding and condition frames.

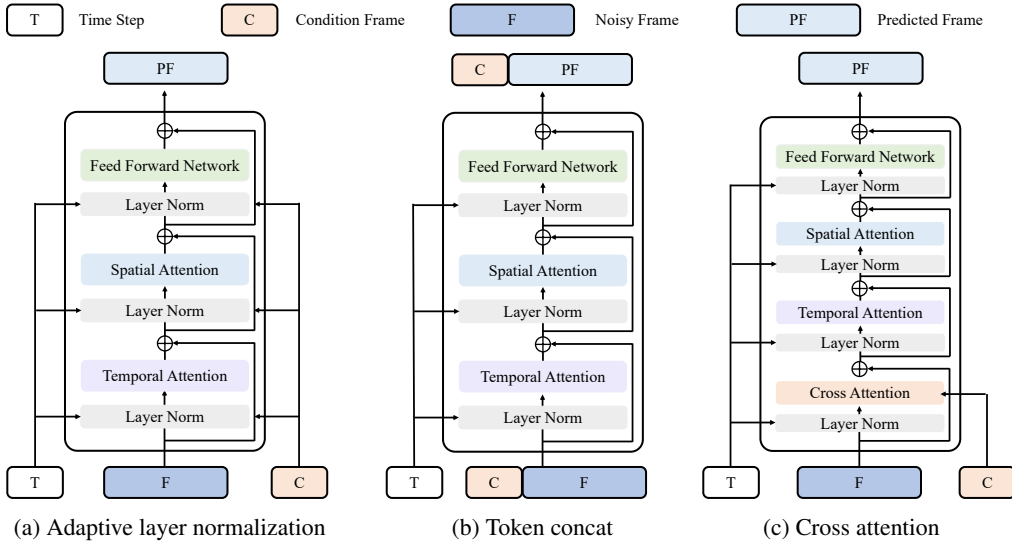


Figure 3: Illustration of three video prediction schemes.

**Cross-attention.** We also explored the use of cross-attention as a video prediction scheme, where the conditional frames are used as keys and values, and the noisy frame serves as the query. This allows for the fusion of conditional information within the noisy frame. Prior to entering the cross-attention layer, the features of the conditional frames are extracted using the VAE tokenizer and being patchified. Spatial and temporal position embeddings are also added to assist our VDT in learning the corresponding information within the conditional frames.

**Token concatenation.** Our VDT model adopts a pure transformer architecture, therefore, a more intuitive approach is to directly utilize conditional frames as input tokens for VDT. We achieve this by concatenating the conditional frames (latent features) and noisy frames in token level, which is then fed into the VDT. Then we split the output frames sequence from VDT and utilize the predicted frames for the diffusion process, as illustrated in Figure 3 (b). We have found that this scheme exhibits the fastest convergence speed as shown in Figure 6, and compared to the previous two approaches, delivers superior results in the final outcomes.

Furthermore, we discovered that even if we use a fixed length for the conditional frames during the training process, our VDT can still take any larger length of conditional frame as input and output consistent predicted features (more details are provided in Appendix).

### 3.3 UNIFIED SPATIAL-TEMPORAL MASK MODELING

In Section 3.2, we demonstrated that simple token concatenation is sufficient to extend VDT to tasks in video prediction. An intuitive question arises: can we further leverage this scalability to extend VDT to more diverse video generation tasks—such as video frame interpolation—into a single, unified model; without introducing any additional modules or parameters.

Reviewing the functionality of our VDT in both unconditional generation and video prediction, the only difference lies in the type of input features. Specifically, the input can either be pure noise latent features or a concatenation of conditions and noise latent features. Then we introduce a conditional spatial-temporal mask to unified the conditional input  $\mathcal{I}$ , as formulated in the following equation:

$$\mathcal{I} = \mathcal{F} \wedge (1 - \mathcal{M}) + \mathcal{C} \wedge \mathcal{M}. \quad (3)$$

Here,  $\mathcal{C} \in R^{F \times H \times W \times C}$  represents the actual conditional video,  $\mathcal{F} \in R^{F \times H \times W \times C}$  signifies noise,  $\wedge$  represents bitwise multiplication, and the spatial-temporal mask  $\mathcal{M} \in R^{F \times H \times W \times C}$  controls whether each token  $t \in R^C$  originates from the real video or noise.

Under this unified framework, we can modulate the the spatial-temporal mask  $\mathcal{M}$  to incorporate additional video generation tasks into the VDT training process. This ensures that a well-trained VDT can be effortlessly applied to various video generation tasks. Specifically, we consider the following training task during the training (as shown in Figure 4 and Figure 5):

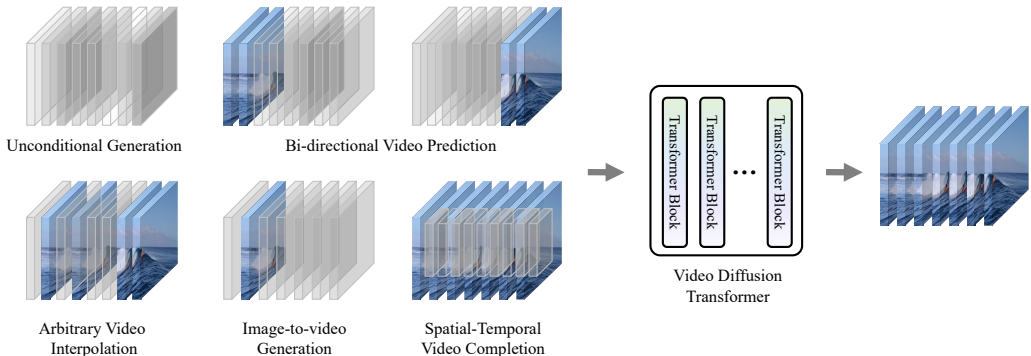


Figure 4: Illustration of our unified spatial-temporal mask modeling mechanism.

**Unconditional Generation** This training task aligns with the procedures outlined in In Section 3.1, where the spatial-temporal  $M$  is set to all zero.

**Bi-directional Video Prediction** Building on our extension of VDT to video prediction tasks in Section 3.2, we further augment the complexity of this task. In addition to traditional forward video prediction, we challenge the model to predict past events based on the final frames of a given video, thereby encouraging enhanced temporal modeling capabilities.

**Arbitrary Video Interpolation** Frame interpolation is a pivotal aspect of video generation. Here, we extend this task to cover scenarios where arbitrary  $n$  frames are given, and the model is required to fill in the missing frames to complete the entire video sequence.

**Image-to-video Generation** is a specific instance of Arbitrary Video Interpolation. Starting from a single image, we random choose a temporal location and force our VDT to generate the full video. Therefore, during inference, we can arbitrarily specify the image’s temporal location and generate a video sequence from it.

**Spatial-Temporal Video Completion** While our previous tasks emphasize temporal modeling, we also delve into extending our model into the spatial domain. With our unified mask modeling mechanism, this is made possible by creating a spatial-temporal mask. However, straightforward random spatial-temporal tasks might be too simple for our VDT since it can easily gather information from surrounding tokens. Drawing inspiration from BEiT (Bao et al., 2021), we adopt a spatial-temporal block mask methodology to preclude the VDT from converging on trivial solutions.

## 4 EXPERIMENT

### 4.1 DATASETS AND SETTINGS.

**Datasets.** The VDT is evaluated on both video generation and video prediction tasks. Unconditional generation results on the widely-used UCF101 (Soomro et al., 2012), TaiChi (Siarohin et al., 2019) and Sky Time-Lapse (Xiong et al., 2018) datasets are provided for video synthesis. For video prediction, experiments are conducted on the real-world driven dataset - Cityscapes (Cordts et al., 2016), as well as on a more challenging physical prediction dataset Physion (Bear et al., 2021) to demonstrate the VDT’s strong prediction ability.

**Evaluation.** We adopt Fréchet Video Distance (FVD) (Unterthiner et al., 2018) as the main metric for comparing our model with previous works, as FVD captures both fidelity and diversity of generated samples. Additionally, for video generation tasks, we report the Structural Similarity Index (SSIM) and Peak Signal-to-Noise Ratio (PSNR). VQA accuracy is reported for the physical prediction task. Consistent with previous work (Voleti et al., 2022), we use clip lengths of 16, 30, and 16 for UCF101, Cityscapes, and Physion, respectively. Furthermore, all videos are center-cropped and downsampled to 64x64 for UCF101, 128x128 for Cityscapes and Physion, 256x256 for TaiChi and Sky Time-Lapse.

**VDT configurations.** In Table 1, we provide detailed information about two versions of the VDT model. By default, we utilize VDT-L for all experiments. We empirically set the initial learning rate to  $1e-4$  and adopt AdamW (Loshchilov & Hutter, 2019) for our training. We utilize a pre-trained

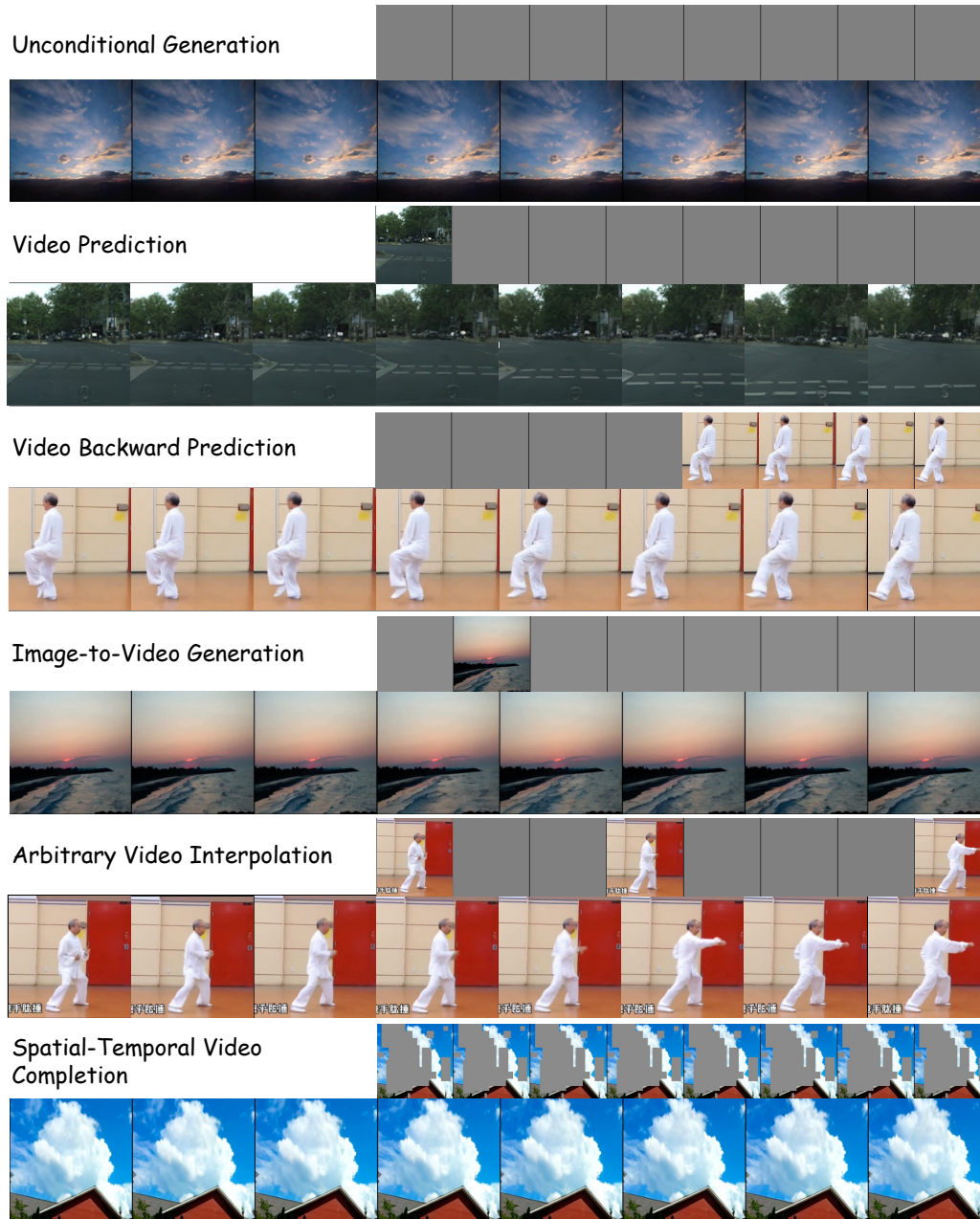


Figure 5: Qualitative results on unified video generation tasks. For each sample, we provide the mask and condition information in the top line, and the result generated by VDT in the bottom.

Table 1: Configurations of VDT. FVD results are reported on UCF101 unconditional generation.

Model	Layer	Hidden State	Heads	MLP ratio	FVD ↓
VDT-S	12	384	6	4	425.6
VDT-L	28	1152	16	4	225.7

variational autoencoder (VAE) model (Rombach et al., 2022) as the tokenizer and freeze it during training. The hyper-parameters are uniformly set to Patchsize = 2. More details are given in Appendix.

## 4.2 ANALYSIS

**Different conditional strategy for video prediction.** In Section 3.2, we explore three conditional strategies: (1) adaptive layer normalization, (2) cross-attention, and (3) token concatenation. The

Table 2: Video prediction on Physion ( $128 \times 128$ ) conditioning on 8 frames and predicting 8. We compare three video prediction schemes.

Methods	FVD ↓	SSIM ↑	PSNR ↑
Ada. LN	270.8	0.6247	16.8
Cross-Attention	134.9	0.8523	28.6
Token Concat	129.1	0.8718	30.2

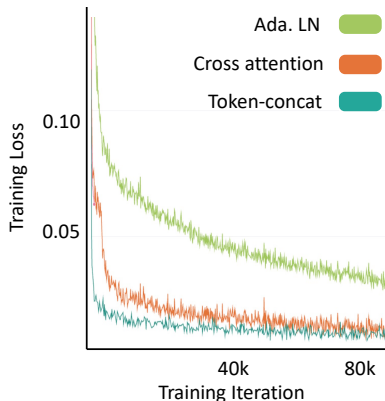
Table 3: Different training strategies of VDT-S on UCF101. S: spatial train only, J: joint train.

Method	S	T	FVD↓	Time
J directly	0	40k	554.8	7.2
J directly	0	80k	451.9	14.4
J directly	0	120k	425.6	21.5
S pre. then J	80k	40k	431.7	11.2

Table 4: Unconditional video generation results on UCF-101. \* means trained on full split (train + test).

Method	Resolution	FVD ↓
<b>GAN:</b>		
TGANv2 (Saito et al., 2020)	$16 \times 128 \times 128$	1209.0
MoCoGAN* (Tulyakov et al., 2018)	$16 \times 128 \times 128$	838.0
DIGAN* (Yu et al., 2022)	$16 \times 128 \times 128$	577.0
<b>Diff. based on U-Net, Large Pre:</b>		
Latent-Shift* (An et al., 2023)	$16 \times 256 \times 256$	360.0
VideoGen* (Li et al., 2023)	$16 \times 256 \times 256$	345.0
VideoFusion* (Luo et al., 2023)	$16 \times 128 \times 128$	220.0
Make-A-Video* (Singer et al., 2022)	$16 \times 256 \times 256$	81.3
<b>Diff. based on U-Net:</b>		
PVDM* (Yu et al., 2023b)	$16 \times 256 \times 256$	343.6
MCVD (Voleti et al., 2022)	$16 \times 64 \times 64$	1143.0
PYoCo* (Ge et al., 2023)	$16 \times 64 \times 64$	310.0
VDM* (Ho et al., 2022b)	$16 \times 64 \times 64$	295.0
<b>Diff. based on Transformer:</b>		
VDT	$16 \times 64 \times 64$	<b>225.7</b>

Figure 6: Training loss on three video prediction schemes. Token concatenation approach achieved the fastest convergence speed and the lowest loss.



results of convergence speed and prediction performance are presented in Figure 3 and Table 2, respectively. Notably, the token concatenation strategy achieves the fastest convergence speed and the best prediction performance (i.e., FVD and SSIM in Table 2). As a result, we adopt the token concatenation strategy for all video prediction tasks in this paper.

**Training strategy.** In this part, we investigate different training strategies in Table 3. For spatial-only training, we remove the temporal attention in each block and sample one frame from each video to force the model to learn the spatial information. This enables the model to focus on learning spatial features separately from temporal features. It is evident that that spatial pretraining then joint training outperforms directly spatial-temporal joint tuning (431.7 vs. 451.9) with significantly less time (11.2 vs. 14.4), indicating the crucial role of image pretraining initialization in video generation.

#### 4.3 COMPARISON TO THE STATE-OF-THE-ARTS

**Unconditional Generation.** The quantitative results in unconditional generation are given in Table 4. Our VDT demonstrates significant superiority over all GAN-based methods. Although MCVD (Voleti et al., 2022) falls under the diffusion-based category, our VDT outperforms it by a significant margin. This difference in performance may be attributed to the fact that MCVD is specifically designed for video prediction tasks. VDM (Ho et al., 2022b) is the most closely related method, as it employs a 2D U-Net with additional temporal attention. However, direct comparisons are not feasible as VDM only presents results on the train+test split. Nevertheless, our VDT achieves superior performance, even with training solely on the train split.

We also conducted a qualitative analysis in Figure 7, focusing on TaiChi (Siarohin et al., 2019) and Sky Time-Lapse (Xiong et al., 2018). It is evident that both DIGAN and VideoFusion exhibit noise artifacts in the Sky scene, whereas our VDT model achieves superior color fidelity. In the TaiChi, DIGAN and VideoFusion predominantly produce static character movements, accompanied by distortions in the hand region. Conversely, our VDT model demonstrates the ability to generate coherent and extensive motion patterns while preserving intricate details.

Table 5: Video prediction on Cityscapes (128 × 128) conditioning on 2 and predicting 28 frames.

Cityscapes	FVD↓	SSIM↑
SVG-LP (Denton & Fergus, 2018)	1300.3	0.574
vRNN IL (Castrejon et al., 2019)	682.1	0.609
Hier-vRNN (Castrejon et al., 2019)	567.5	0.628
GHVAE (Wu et al., 2021)	418.0	0.740
MCVD-spatin (Voleti et al., 2022)	184.8	0.720
MCVD-concat (Voleti et al., 2022)	<b>141.4</b>	0.690
VDT	142.3	<b>0.880</b>

Table 6: VQA accuracy on Physion-Collide.

Model	Accuracy
<b>Object centric:</b>	
Human (upper bound)	80.0
SlotFormer (Wu et al., 2022b)	69.3
<b>Scene centric:</b>	
PRIN (Qi et al., 2021)	57.9
pVGG-lstm (Bear et al., 2021)	58.7
pDEIT-lstm (Bear et al., 2021)	63.1
<b>VDT (Ours)</b>	<b>65.3</b>

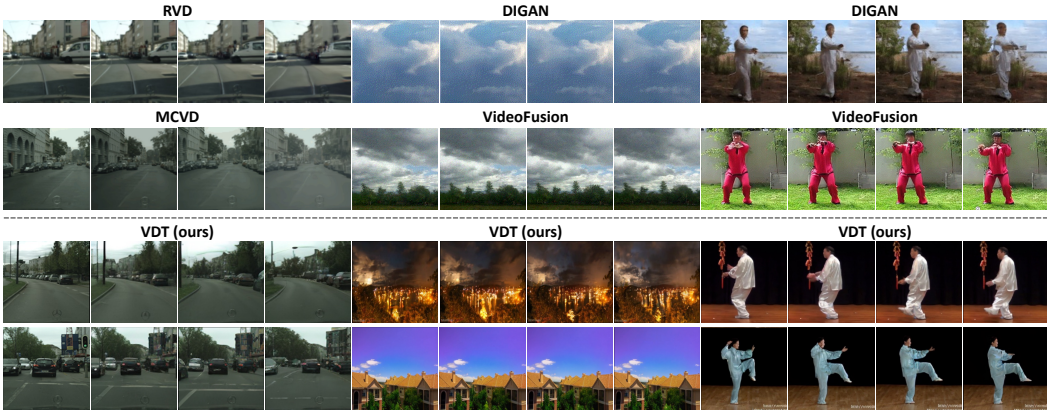


Figure 7: Qualitative video results on video prediction tasks (Cityscapes, 128 × 128) and video generation tasks (TaiChi-HD and Sky Time-Lapse, 256 × 256).

**Video Prediction.** Video Prediction is another crucial task in video diffusion. Different from previous works (Voleti et al., 2022) specially designing a diffusion-based architecture to adopt 2D U-Net in video prediction task, the inherent sequence modeling capability of transformers allows our VDT for seamless extension to video prediction tasks. We evaluate it on the Cityscape dataset in Table 5 and Figure 7. It can be observed that our VDT is comparable to MCVD (Voleti et al., 2022) in terms of FVD and superior in terms of SSIM, although we employ a straightforward token concatenation strategy. Additionally, we observe that existing prediction methods often suffer from brightness and color shifts during the prediction process as shown in Figure 7. However, our VDT maintains remarkable overall color consistency in the generated videos. These findings demonstrate the impressive video prediction capabilities of VDT.

**Physical Video Prediction.** We further evaluate our VDT model on the highly challenging Physion dataset. Physion is a physical prediction dataset, specifically designed to assess a model’s capability to forecast the temporal evolution of physical scenarios. In contrast to previous object-centric approaches that involve extracting objects and subsequently modeling the physical processes, our VDT tackles the video prediction task directly. It effectively learns the underlying physical phenomena within the conditional frames while generating accurate video predictions. We conducted a VQA test following the official approach, as shown in Table 6. In this test, a simple MLP is applied to the observed frames and the predicted frames to determine whether two objects collide. Our VDT model outperforms all scene-centric methods in this task. These results provide strong evidence of the impressive physical video prediction capabilities of our VDT model.

## 5 CONCLUSION

In this paper, we introduce the Video Diffusion Transformer (VDT), a video generation model based on a simple yet effective transformer architecture. The inherent sequence modeling capability of transformers allows for seamless extension to video prediction tasks using a straightforward token concatenation strategy. Our experimental evaluation, both quantitatively and qualitatively, demonstrates the remarkable potential of the VDT in advancing the field of video generation. We believe our work will serve as an inspiration for future research in the field of video generation.

## ACKNOWLEDGEMENTS

This work was supported by National Natural Science Foundation of China (62376274).

## REFERENCES

- Jie An, Songyang Zhang, Harry Yang, Sonal Gupta, Jia-Bin Huang, Jiebo Luo, and Xi Yin. Latent-shift: Latent diffusion with temporal shift for efficient text-to-video generation. *arXiv preprint arXiv:2304.08477*, 2023.
- Fan Bao, Chongxuan Li, Yue Cao, and Jun Zhu. All are worth words: a vit backbone for score-based diffusion models. *arXiv preprint arXiv:2209.12152*, 2022.
- Hangbo Bao, Li Dong, and Furu Wei. BEiT: BERT pre-training of image transformers. *arXiv preprint arXiv:2106.08254*, 2021.
- Daniel Bear, Elias Wang, Damian Mrowca, Felix J. Binder, Hsiao-Yu Tung, R. T. Pramod, Cameron Holdaway, Sirui Tao, Kevin A. Smith, Fan-Yun Sun, Fei-Fei Li, Nancy Kanwisher, Josh Tenenbaum, Dan Yamins, and Judith E. Fan. Physion: Evaluating physical prediction from vision in humans and machines. In *NeurIPS, Datasets and Benchmarks*, 2021.
- Andreas Blattmann, Robin Rombach, Huan Ling, Tim Dockhorn, Seung Wook Kim, Sanja Fidler, and Karsten Kreis. Align your latents: High-resolution video synthesis with latent diffusion models. *arXiv preprint arXiv:2304.08818*, 2023.
- Lluís Castrejon, Nicolas Ballas, and Aaron Courville. Improved conditional vrns for video prediction. In *CVPR*, pp. 7608–7617, 2019.
- Jooyoung Choi, Sungwon Kim, Yonghyun Jeong, Youngjune Gwon, and Sungroh Yoon. ILVR: Conditioning method for denoising diffusion probabilistic models. In *ICCV*, pp. 14347–14356, 2021.
- Marius Cordts, Mohamed Omran, Sebastian Ramos, Timo Rehfeld, Markus Enzweiler, Rodrigo Benenson, Uwe Franke, Stefan Roth, and Bernt Schiele. The cityscapes dataset for semantic urban scene understanding. In *CVPR*, pp. 3213–3223, 2016.
- Emily Denton and Rob Fergus. Stochastic video generation with a learned prior. In *ICML*, pp. 1174–1183. PMLR, 2018.
- Prafulla Dhariwal and Alexander Quinn Nichol. Diffusion models beat GANs on image synthesis. In *NeurIPS*, pp. 8780–8794, 2021.
- Alexey Dosovitskiy, Lucas Beyer, Alexander Kolesnikov, Dirk Weissenborn, Xiaohua Zhai, Thomas Unterthiner, Mostafa Dehghani, Matthias Minderer, Georg Heigold, Sylvain Gelly, Jakob Uszkoreit, and Neil Houlsby. An image is worth 16x16 words: Transformers for image recognition at scale. In *ICLR*, 2021.
- Patrick Esser, Robin Rombach, and Björn Ommer. Taming transformers for high-resolution image synthesis. In *CVPR*, pp. 12873–12883, 2021.
- Patrick Esser, Johnathan Chiu, Parmida Atighehchian, Jonathan Granskog, and Anastasis Germanidis. Structure and content-guided video synthesis with diffusion models. *arXiv preprint arXiv:2302.03011*, 2023.
- Songwei Ge, Thomas Hayes, Harry Yang, Xi Yin, Guan Pang, David Jacobs, Jia-Bin Huang, and Devi Parikh. Long video generation with time-agnostic VQGAN and time-sensitive transformer. In Shai Avidan, Gabriel J. Brostow, Moustapha Cissé, Giovanni Maria Farinella, and Tal Hassner (eds.), *ECCV*, pp. 102–118, 2022.
- Songwei Ge, Seungjun Nah, Guilin Liu, Tyler Poon, Andrew Tao, Bryan Catanzaro, David Jacobs, Jia-Bin Huang, Ming-Yu Liu, and Yogesh Balaji. Preserve your own correlation: A noise prior for video diffusion models. *arXiv preprint arXiv:2305.10474*, 2023.

- Agrim Gupta, Stephen Tian, Yunzhi Zhang, Jiajun Wu, Roberto Martín-Martín, and Li Fei-Fei. Maskvit: Masked visual pre-training for video prediction. In *ICLR*, 2023.
- Yingqing He, Tianyu Yang, Yong Zhang, Ying Shan, and Qifeng Chen. Latent video diffusion models for high-fidelity long video generation. *arXiv preprint arXiv:2211.13221*, 2022.
- Jonathan Ho and Tim Salimans. Classifier-free diffusion guidance. *arXiv preprint arXiv:2207.12598*, 2022.
- Jonathan Ho, Ajay Jain, and Pieter Abbeel. Denoising diffusion probabilistic models. In *NeurIPS*, pp. 6840–6851, 2020.
- Jonathan Ho, William Chan, Chitwan Saharia, Jay Whang, Ruiqi Gao, Alexey Gritsenko, Diederik P Kingma, Ben Poole, Mohammad Norouzi, David J Fleet, et al. Imagen video: High definition video generation with diffusion models. *arXiv preprint arXiv:2210.02303*, 2022a.
- Jonathan Ho, Tim Salimans, Alexey Gritsenko, William Chan, Mohammad Norouzi, and David J Fleet. Video diffusion models. *arXiv preprint arXiv:2204.03458*, 2022b.
- Rongjie Huang, Jiawei Huang, Dongchao Yang, Yi Ren, Luping Liu, Mingze Li, Zhenhui Ye, Jinglin Liu, Xiang Yin, and Zhou Zhao. Make-an-audio: Text-to-audio generation with prompt-enhanced diffusion models. *arXiv preprint arXiv:2301.12661*, 2023.
- Zhifeng Kong, Wei Ping, Jiaji Huang, Kexin Zhao, and Bryan Catanzaro. Diffwave: A versatile diffusion model for audio synthesis. *arXiv preprint arXiv:2009.09761*, 2020.
- Xin Li, Wenqing Chu, Ye Wu, Weihang Yuan, Fanglong Liu, Qi Zhang, Fu Li, Haocheng Feng, Errui Ding, and Jingdong Wang. Videogen: A reference-guided latent diffusion approach for high definition text-to-video generation. *arXiv preprint arXiv:2309.00398*, 2023.
- Ilya Loshchilov and Frank Hutter. Decoupled weight decay regularization. In *ICLR*, 2019. URL <https://openreview.net/forum?id=Bkg6RiCqY7>.
- Haoyu Lu, Mingyu Ding, Nanyi Fei, Yuqi Huo, and Zhiwu Lu. Lgdn: Language-guided denoising network for video-language modeling. *arXiv preprint arXiv:2209.11388*, 2022.
- Shitong Luo and Wei Hu. Diffusion probabilistic models for 3d point cloud generation. In *CVPR*, pp. 2837–2845, 2021.
- Zhengxiong Luo, Dayou Chen, Yingya Zhang, Yan Huang, Liang Wang, Yujun Shen, Deli Zhao, Jinren Zhou, and Tieniu Tan. Decomposed diffusion models for high-quality video generation. *arXiv preprint arXiv:2303.08320*, 2023.
- Sharan Narang and Aakanksha Chowdhery. Pathways language model (palm): Scaling to 540 billion parameters for breakthrough performance. *Google AI Blog*, 2022.
- Alexander Quinn Nichol and Prafulla Dhariwal. Improved denoising diffusion probabilistic models. In *ICML*, volume 139, pp. 8162–8171, 2021.
- William Peebles and Saining Xie. Scalable diffusion models with transformers. *arXiv preprint arXiv:2212.09748*, 2022.
- Dustin Podell, Zion English, Kyle Lacey, Andreas Blattmann, Tim Dockhorn, Jonas Müller, Joe Penna, and Robin Rombach. Sdxl: improving latent diffusion models for high-resolution image synthesis. *arXiv preprint arXiv:2307.01952*, 2023.
- Haozhi Qi, Xiaolong Wang, Deepak Pathak, Yi Ma, and Jitendra Malik. Learning long-term visual dynamics with region proposal interaction networks. In *ICLR*, 2021.
- Aditya Ramesh, Prafulla Dhariwal, Alex Nichol, Casey Chu, and Mark Chen. Hierarchical text-conditional image generation with clip latents. *arXiv preprint arXiv:2204.06125*, 2022.
- Robin Rombach, Andreas Blattmann, Dominik Lorenz, Patrick Esser, and Björn Ommer. High-resolution image synthesis with latent diffusion models. *arXiv preprint arXiv:2112.10752*, 2021.

- Robin Rombach, Andreas Blattmann, Dominik Lorenz, Patrick Esser, and Björn Ommer. High-resolution image synthesis with latent diffusion models. In *CVPR*, pp. 10684–10695, 2022.
- Olaf Ronneberger, Philipp Fischer, and Thomas Brox. U-net: Convolutional networks for biomedical image segmentation. In *MICCAI*, pp. 234–241. Springer, 2015.
- Masaki Saito, Eiichi Matsumoto, and Shunta Saito. Temporal generative adversarial nets with singular value clipping. In *ICCV*, pp. 2830–2839, 2017.
- Masaki Saito, Shunta Saito, Masanori Koyama, and Sosuke Kobayashi. Train sparsely, generate densely: Memory-efficient unsupervised training of high-resolution temporal GAN. *Int. J. Comput. Vis.*, pp. 2586–2606, 2020.
- Aliaksandr Siarohin, Stéphane Lathuilière, Sergey Tulyakov, Elisa Ricci, and Nicu Sebe. First order motion model for image animation. *NeurIPS*, 32, 2019.
- Uriel Singer, Adam Polyak, Thomas Hayes, Xi Yin, Jie An, Songyang Zhang, Qiyuan Hu, Harry Yang, Oron Ashual, Oran Gafni, et al. Make-a-video: Text-to-video generation without text-video data. *arXiv preprint arXiv:2209.14792*, 2022.
- Jascha Sohl-Dickstein, Eric A. Weiss, Niru Maheswaranathan, and Surya Ganguli. Deep unsupervised learning using nonequilibrium thermodynamics. In *ICML*, volume 37, pp. 2256–2265, 2015.
- Jiaming Song, Chenlin Meng, and Stefano Ermon. Denoising diffusion implicit models. In *ICLR*, 2021.
- Yang Song and Stefano Ermon. Generative modeling by estimating gradients of the data distribution. In *NeurIPS*, pp. 11895–11907, 2019.
- Khurram Soomro, Amir Roshan Zamir, and Mubarak Shah. Ucf101: A dataset of 101 human actions classes from videos in the wild. *arXiv preprint arXiv:1212.0402*, 2012.
- Sergey Tulyakov, Ming-Yu Liu, Xiaodong Yang, and Jan Kautz. Mocogan: Decomposing motion and content for video generation. In *ICCV*, pp. 1526–1535, 2018.
- Thomas Unterthiner, Sjoerd Van Steenkiste, Karol Kurach, Raphael Marinier, Marcin Michalski, and Sylvain Gelly. Towards accurate generative models of video: A new metric & challenges. *arXiv preprint arXiv:1812.01717*, 2018.
- Vikram Voleti, Alexia Jolicoeur-Martineau, and Christopher Pal. Masked conditional video diffusion for prediction, generation, and interpolation. *arXiv preprint arXiv:2205.09853*, 2022.
- Carl Vondrick, Hamed Pirsiavash, and Antonio Torralba. Generating videos with scene dynamics. *NeurIPS*, 29, 2016.
- Junke Wang, Dongdong Chen, Zuxuan Wu, Chong Luo, Luowei Zhou, Yucheng Zhao, Yujia Xie, Ce Liu, Yu-Gang Jiang, and Lu Yuan. Omnivl: One foundation model for image-language and video-language tasks. *arXiv preprint arXiv:2209.07526*, 2022a.
- Limin Wang, Bingkun Huang, Zhiyu Zhao, Zhan Tong, Yanan He, Yi Wang, Yali Wang, and Yu Qiao. Videomae v2: Scaling video masked autoencoders with dual masking. *arXiv preprint arXiv:2303.16727*, 2023a.
- Wenjing Wang, Huan Yang, Zixi Tuo, Huiguo He, Junchen Zhu, Jianlong Fu, and Jiaying Liu. Videofactory: Swap attention in spatiotemporal diffusions for text-to-video generation. *arXiv preprint arXiv:2305.10874*, 2023b.
- Xiang Wang, Hangjie Yuan, Shiwei Zhang, Dayou Chen, Jiuniu Wang, Yingya Zhang, Yujun Shen, Deli Zhao, and Jingren Zhou. Videocomposer: Compositional video synthesis with motion controllability. *arXiv preprint arXiv:2306.02018*, 2023c.
- Yi Wang, Kunchang Li, Yizhuo Li, Yanan He, Bingkun Huang, Zhiyu Zhao, Hongjie Zhang, Jilan Xu, Yi Liu, Zun Wang, et al. Internvideo: General video foundation models via generative and discriminative learning. *arXiv preprint arXiv:2212.03191*, 2022b.

- Bohan Wu, Suraj Nair, Roberto Martín-Martín, Li Fei-Fei, and Chelsea Finn. Greedy hierarchical variational autoencoders for large-scale video prediction. In *CVPR*, pp. 2318–2328, 2021.
- Jay Zhangjie Wu, Yixiao Ge, Xintao Wang, Stan Weixian Lei, Yuchao Gu, Wynne Hsu, Ying Shan, Xiaohu Qie, and Mike Zheng Shou. Tune-a-video: One-shot tuning of image diffusion models for text-to-video generation. *arXiv preprint arXiv:2212.11565*, 2022a.
- Ziyi Wu, Nikita Dvornik, Klaus Greff, Thomas Kipf, and Animesh Garg. Slotformer: Unsupervised visual dynamics simulation with object-centric models. *arXiv preprint arXiv:2210.05861*, 2022b.
- Wei Xiong, Wenhan Luo, Lin Ma, Wei Liu, and Jiebo Luo. Learning to generate time-lapse videos using multi-stage dynamic generative adversarial networks. In *CVPR*, pp. 2364–2373, 2018.
- Ruihan Yang, Prakhara Srivastava, and Stephan Mandt. Diffusion probabilistic modeling for video generation. *arXiv preprint arXiv:2203.09481*, 2022.
- Lijun Yu, Yong Cheng, Kihyuk Sohn, José Lezama, Han Zhang, Huiwen Chang, Alexander G Hauptmann, Ming-Hsuan Yang, Yuan Hao, Irfan Essa, et al. Magvit: Masked generative video transformer. In *CVPR*, pp. 10459–10469, 2023a.
- Sihyun Yu, Jihoon Tack, Sangwoo Mo, Hyunsu Kim, Junho Kim, Jung-Woo Ha, and Jinwoo Shin. Generating videos with dynamics-aware implicit generative adversarial networks. *arXiv preprint arXiv:2202.10571*, 2022.
- Sihyun Yu, Kihyuk Sohn, Subin Kim, and Jinwoo Shin. Video probabilistic diffusion models in projected latent space. In *CVPR*, pp. 18456–18466, 2023b.
- Chen-Lin Zhang, Jianxin Wu, and Yin Li. Actionformer: Localizing moments of actions with transformers. In *ECCV*, pp. 492–510, 2022.

Table 7: Ablation study on patch size.

Patch	GFlops	FVD
4	1.9	643.9
2	7.7	554.8
1	30.9	466.2

Table 8: Ablation study on attention head.

Head	GFlops	FVD
3	7.7	559.8
6	7.7	554.8
12	7.7	598.7

Table 9: Ablation study on layer.

Layer	GFlops	FVD
6	3.9	580.7
12	7.7	554.8
18	11.6	500.6

Table 10: Ablation study on hidden size.

Hidden Size	GFlops	FVD
192	1.9	704.2
384	7.7	554.8
768	30.9	464.2

Table 11: Ablation study on architecture.

Architecture	GFlops	FVD
Spatial First	7.7	550.2
Temporal First	7.7	554.8

**Limitation and broader impacts.** Due to the limitations of our GPU computing resources, we were unable to pretrain our VDT model on large-scale image or video datasets, which restricts its potential. In future research, we aim to address this limitation by conducting pretraining on larger datasets. Furthermore, we plan to explore the incorporation of other modalities, such as text, into our VDT model. For video generation, it is essential to conduct a thorough analysis of the potential consequences and adopt responsible practices to address any negative impacts.

## A ADDITIONAL ABLATION STUDY

In this part, we conduct a detailed ablation study on UCF101 with VDT-S in Table 7, 8, 9, 10, 11. The results show that reducing the Patchsize, increasing the number of Layers, and increasing the Hidden Size all further improve the model’s performance. The position of Temporal and Spatial attention and the number of attention heads do not significantly affect the model’s results. Further comprehensive analysis indicates that generally, **an increase in GFlops leads to better results, demonstrating the scalability of VDT**. When maintaining the same GFlops, some trade-offs in design are necessary, but overall, the model’s performance does not differ significantly.

## B TRAINING AND INFERENCE COST

We list training and inference times in Table 12, all experiments are conducted on NVIDIA A100 GPUs.

## C DETAILS OF DOWNSTREAM TASKS

We list hyperparameters and training details for downstream tasks in Table 13.

## D PHYSICAL VIDEO PREDICTION.

Most video prediction task was designed based on a limited number of short frames to predict the subsequent video sequence. However, in many complex real-world scenarios, the conditioning information can be highly intricate and cannot be adequately summarized by just a few frames. As a result, it becomes crucial for the model to possess a comprehensive understanding of the conditioning information in order to accurately generate prediction frames while maintaining semantic coherence.

Table 12: Training and inference times (per sample).

	Resolution	VAE	Training	Inference (t=256)
VDT-S	64x64	0.0042	0.022	1.10
VDT-L	64x64	0.0042	0.051	2.57
VDT-S	128x128	0.0051	0.024	1.21
VDT-L	128x128	0.0051	0.057	6.3
VDT-S	256x256	0.0058	0.026	2.63
VDT-L	256x256	0.0058	0.111	25.31

## VideoFusion



## VDT (ours)



Figure 8: Qualitative results on TaiChi-HD.

Therefore, we further evaluate our VDT model on the highly challenging Physion dataset. Physion is a physical prediction dataset, specifically designed to assess a model’s capability to forecast the temporal evolution of physical scenarios. It offers a more comprehensive and demanding benchmark compared to previous datasets. In contrast to previous object-centric approaches that involve extracting objects and subsequently modeling the physical processes, our VDT tackles the video prediction task directly. It effectively learns the underlying physical phenomena within the conditional frames while generating accurate video predictions.

Specifically, we uniformly sample 8 frames from the observed set of each video as conditional frames and predict the subsequent 8 frames for physical prediction. We present qualitative results in Figure 17 to showcase the quality of our predictions. Our VDT exhibits a strong understanding of the underlying physical processes in different samples, which demonstrates a comprehensive understanding of conditional physical information. Meanwhile, our VDT maintains a high level of

Table 13: Hyperparameters for each task.

Config	Unconditional Generation			Video Prediction	
	UCF101	Sky Time-Lapse	TaiChi	CityScapes	Physion
optimizer	AdamW	AdamW	AdamW	AdamW	AdamW
weight decay	0	0	0	0	0
learning rate	1e-4	1e-4	1e-4	1e-4	1e-4
diffusion noise schedule	linear	linear	linear	linear	linear
EMA	0.9999	0.9999	0.9999	0.9999	0.9999
batch size (stage 1)	256	256	256	128	128
batch size (stage 2)	128	64	64	32	32
training resolution	16x64x64	16x256x256	16x256x256	16x128x128	16x128x128
inference resolution	16x64x64	16x256x256	16x256x256	16x128x128	16x128x128
frameskip	1	1	1	1	3

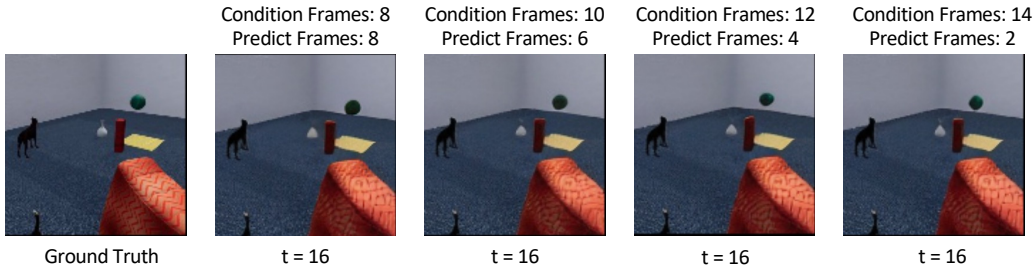


Figure 9: Video prediction results (16x128x128) of frame 16th on the Physion dataset (Bear et al., 2021). During training, we utilize 8 frames as conditional frames and predict the subsequent 8 frames. Then we zero-shot transfer our VDT to condition frames of different larger sizes during inference. We observe that our VDT can perfectly generalize to downstream tasks of different lengths without any additional training.

semantic consistency. Furthermore, we also conducted a VQA test following the official approach, as shown in Table 6. In this test, a simple MLP is applied to the observed frames and the predicted frames to determine whether two objects collide. Our VDT model outperforms all scene-centric methods in this task. These results provide strong evidence of the impressive physical video prediction capabilities of our VDT model.

## E ZERO-SHOT ADAPTATION TO LONGER CONDITIONAL FRAMES

In our experiment, we find that despite training our VDT (Variable Duration Transformer) with fixed-length condition frames, during the inference process, our VDT can zero-shot transfer to condition frames of different sizes. We illustrate this example in Figure 19 and Figure 9. In training, the condition frames were set to a fixed length of 8. However, during inference, we selected condition frames of lengths 8, 10, 12, and 14, and we observed that the model could perfectly generalize to downstream tasks of different lengths without any additional training. Moreover, the model naturally learned additional information from the extended condition frames. As shown in Figure 9, the prediction of the sample with conditional frame length 14 is more accurate at the 16th frame compared to the sample with conditional frame length 8.

## F MORE QUALITATIVE RESULTS

We provide more qualitative results in Figure 10, 11, 12, 13, 14, 15, 16, 17, 18, 19, 18, and 21.

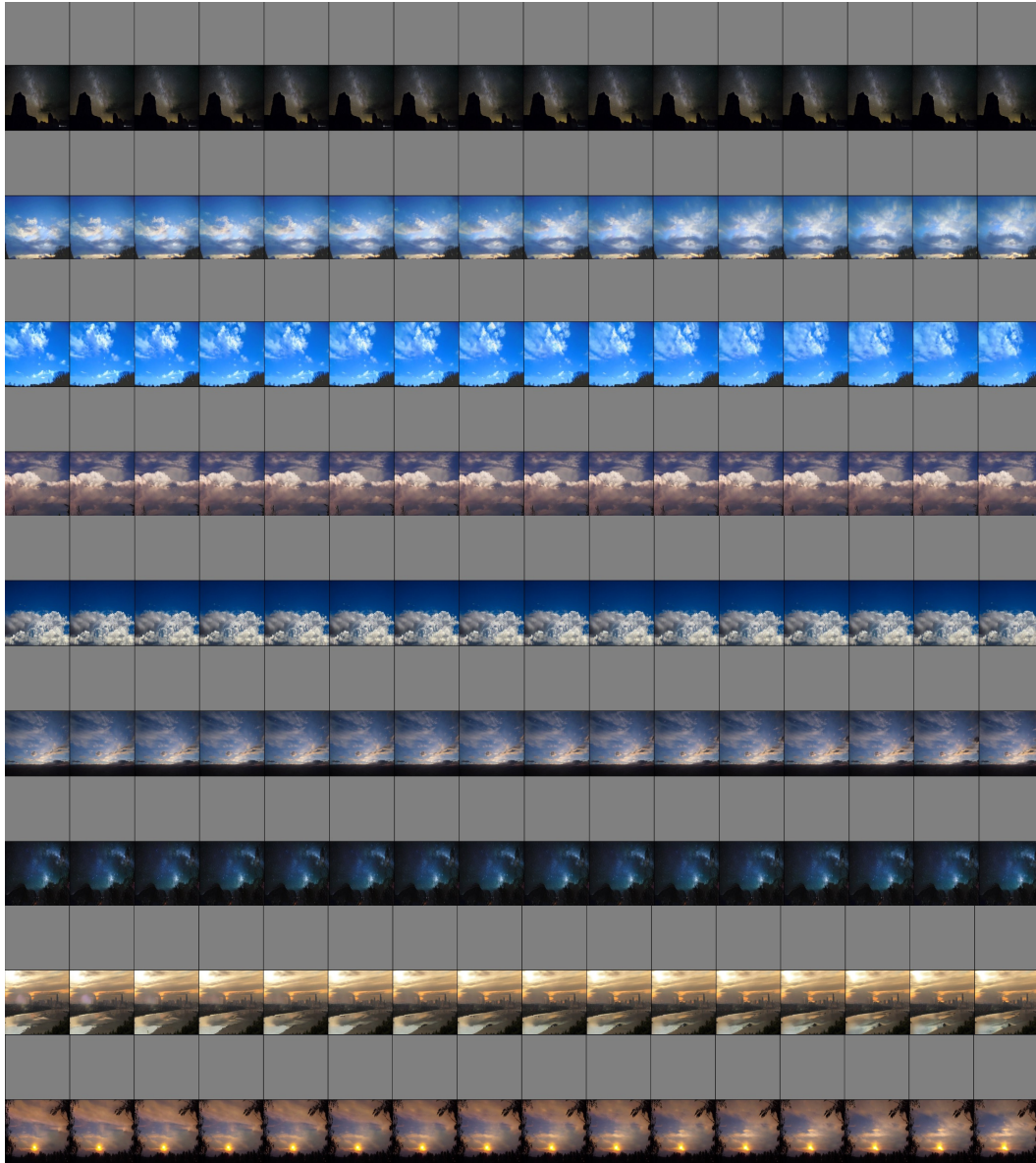


Figure 10: Qualitative results (16x256x256) on Sky Time-Lapse.

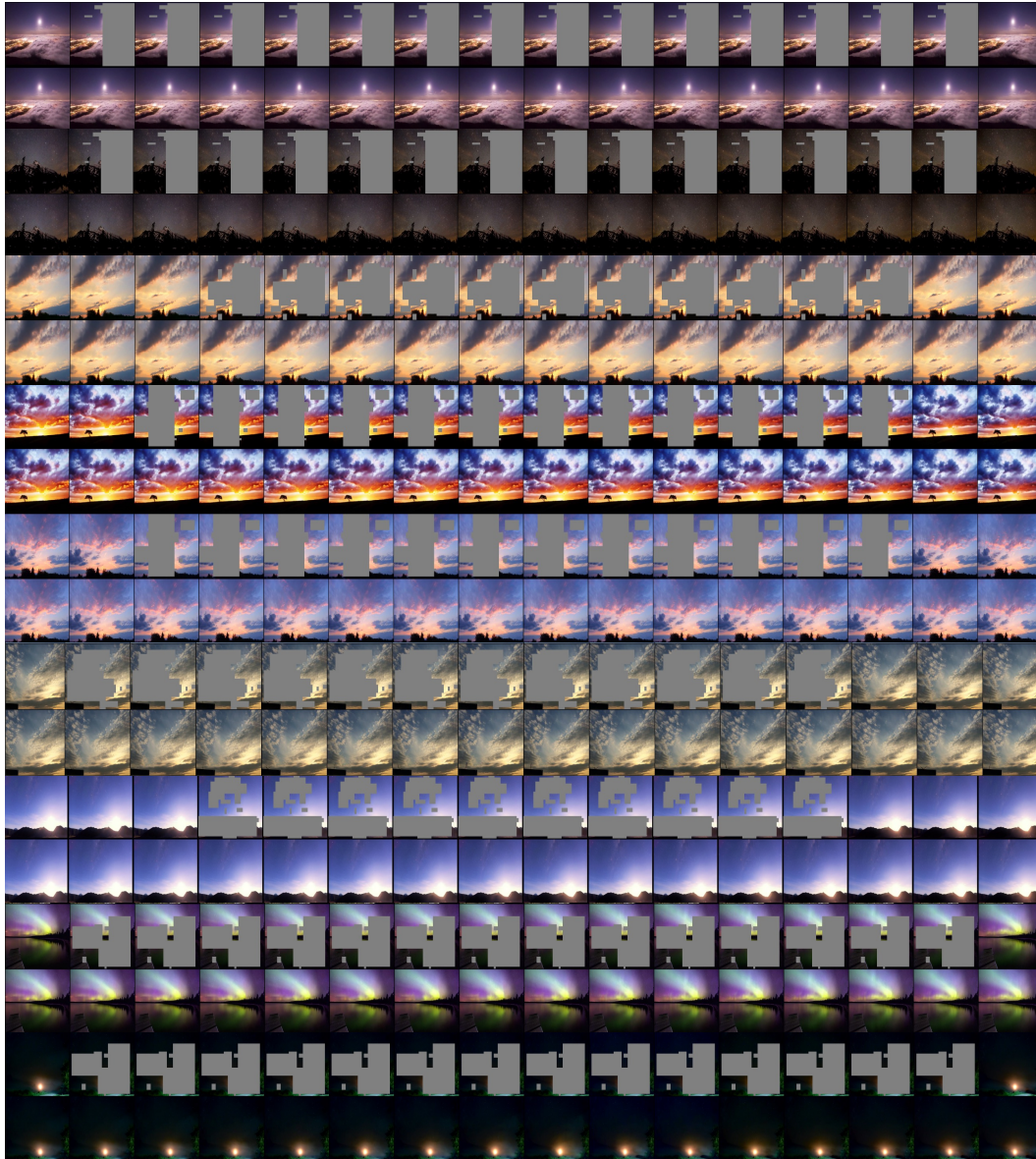


Figure 11: Qualitative results (16x256x256) on Sky Time-Lapse.

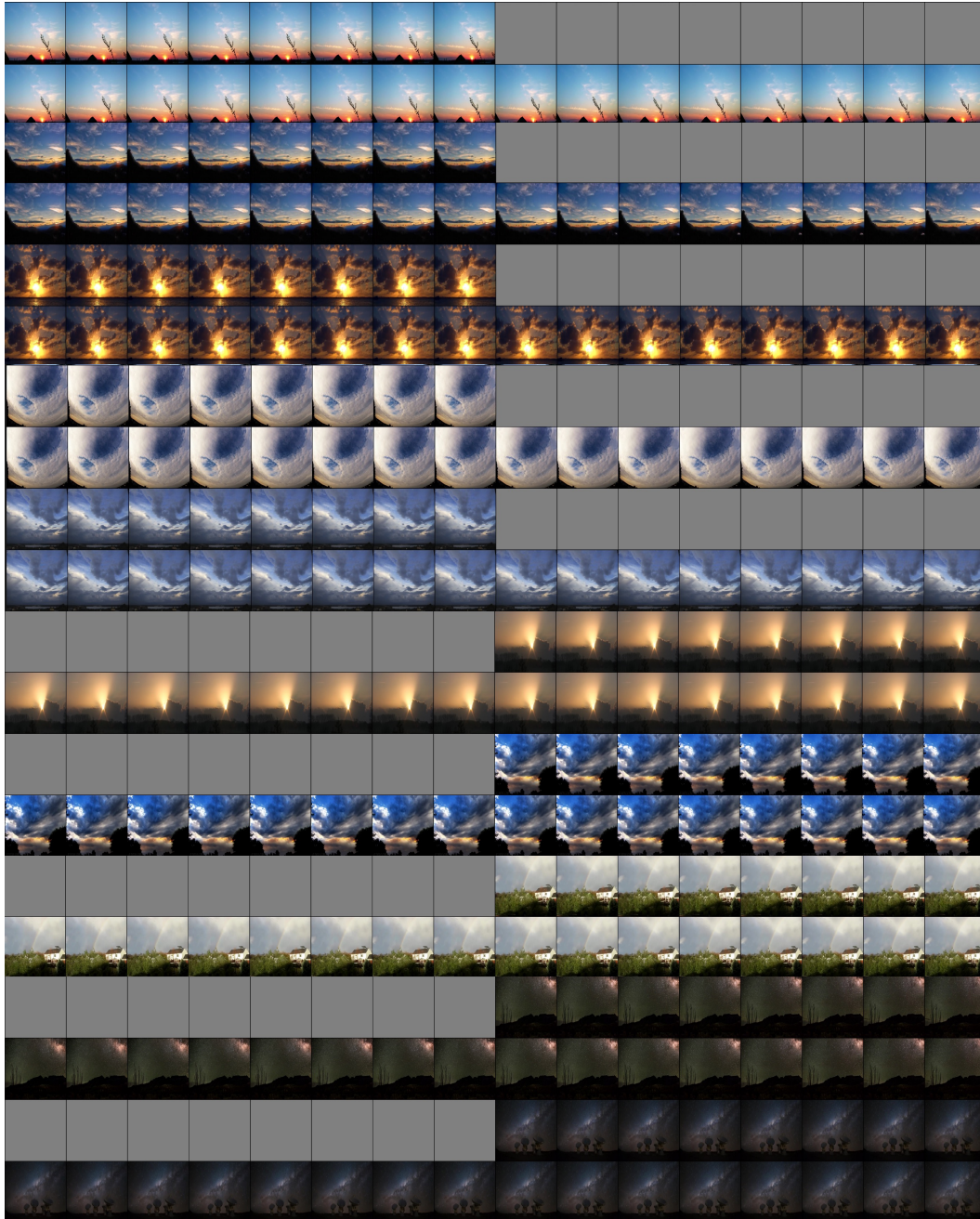


Figure 12: Qualitative results (16x256x256) on Sky Time-Lapse.

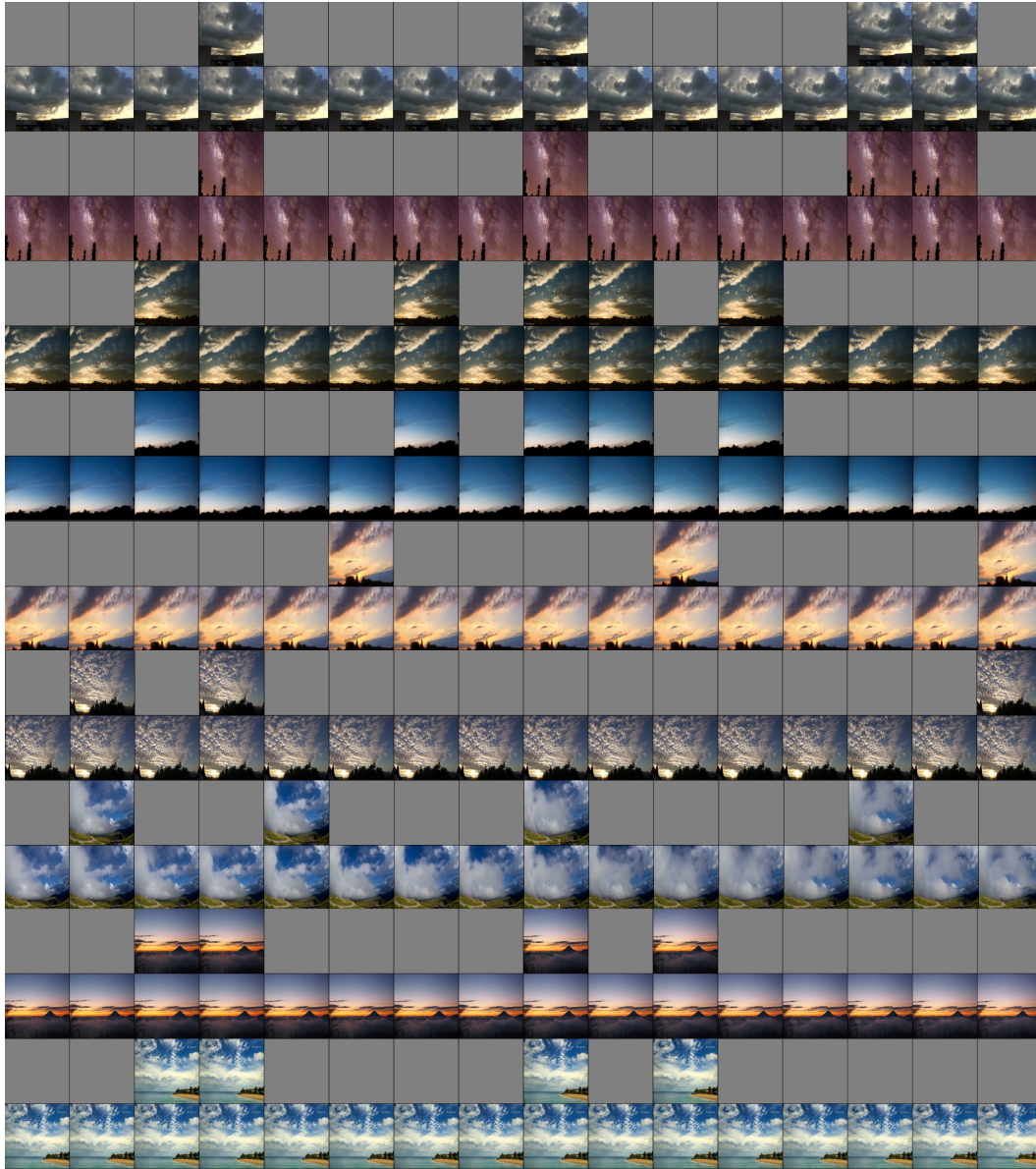


Figure 13: Qualitative results (16x256x256) on Sky Time-Lapse.

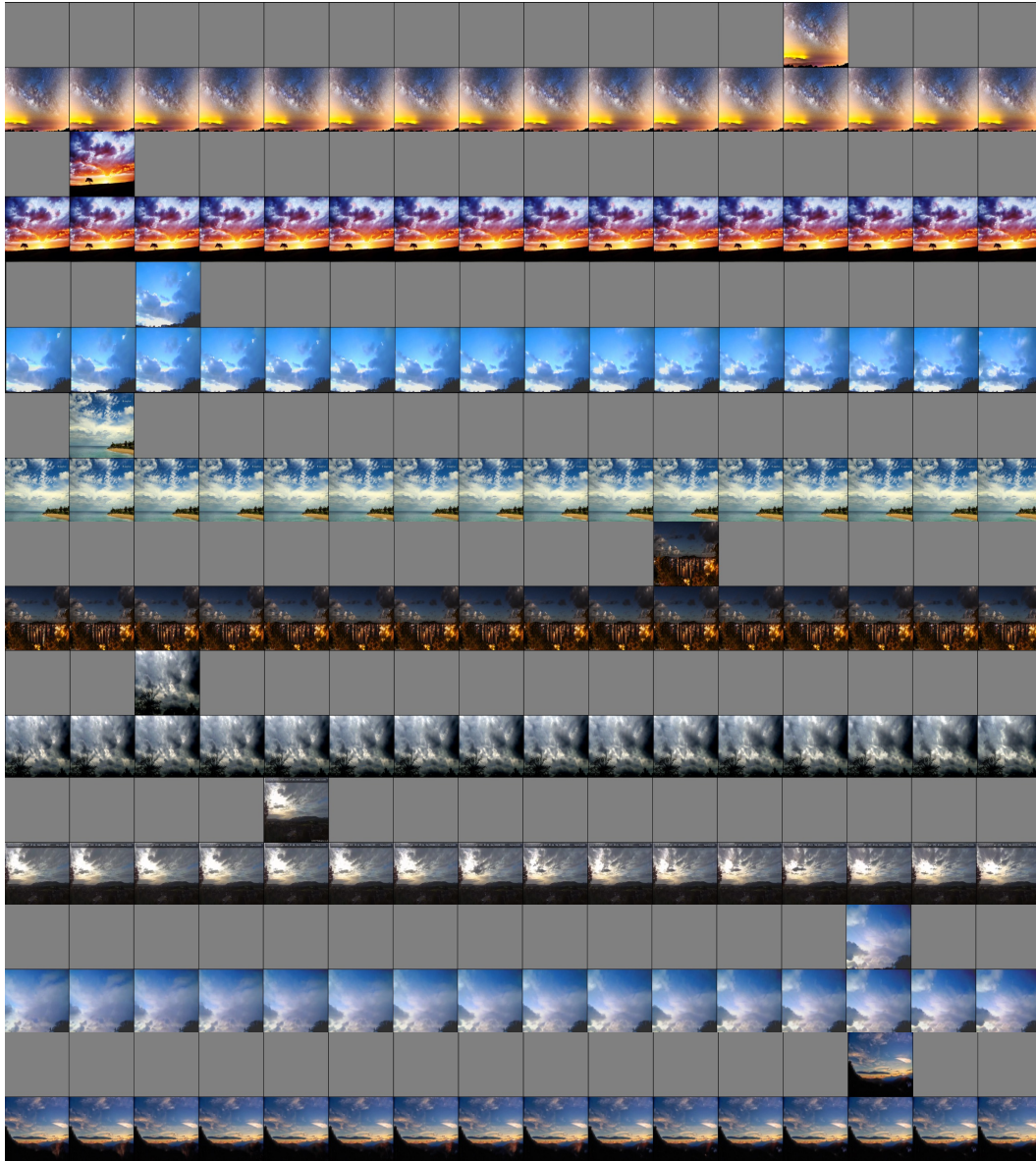


Figure 14: Qualitative results (16x256x256) on Sky Time-Lapse.



Figure 15: Qualitative results (16x256x256) on TaiChi-HD.

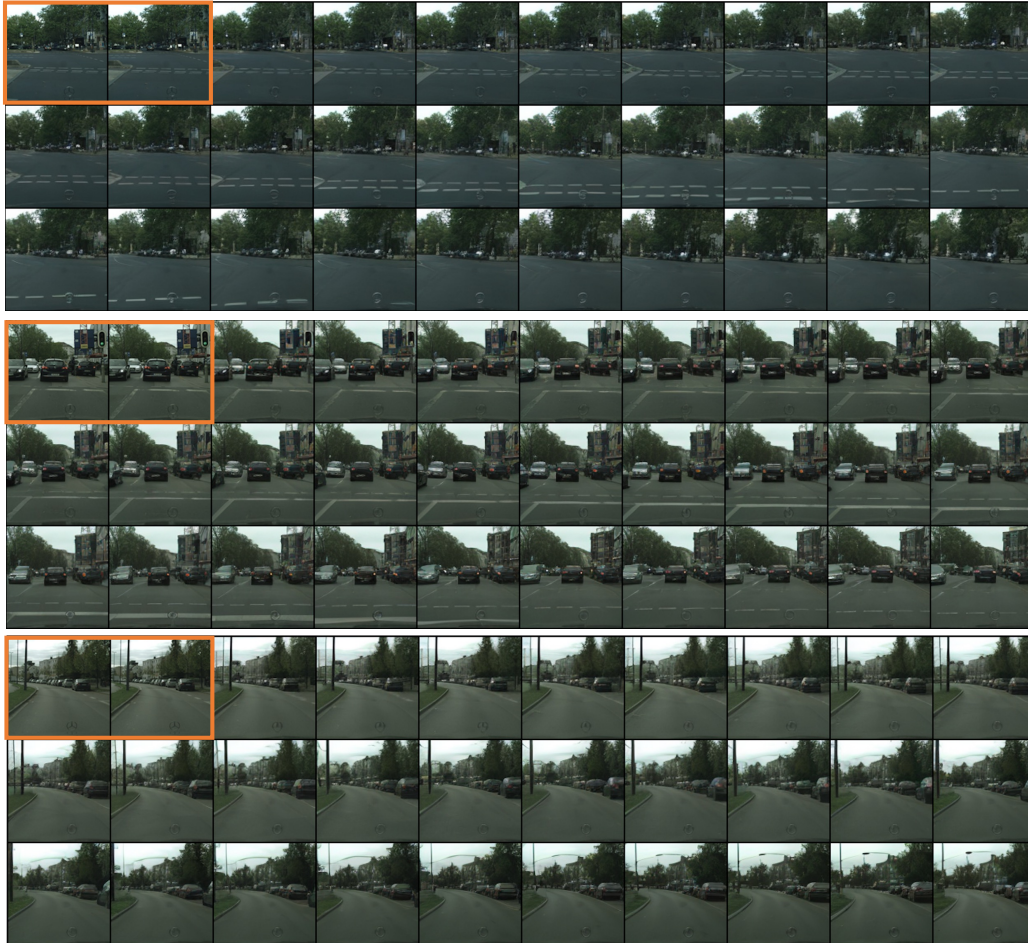


Figure 16: Qualitative video prediction results on Cityscapes (16x128x128), where we utilize 2 frames as conditional frames and predict the subsequent 28 frames in a single forward pass. The predicted frames exhibit semantic coherence, maintaining a high level of consistency in terms of color and brightness.

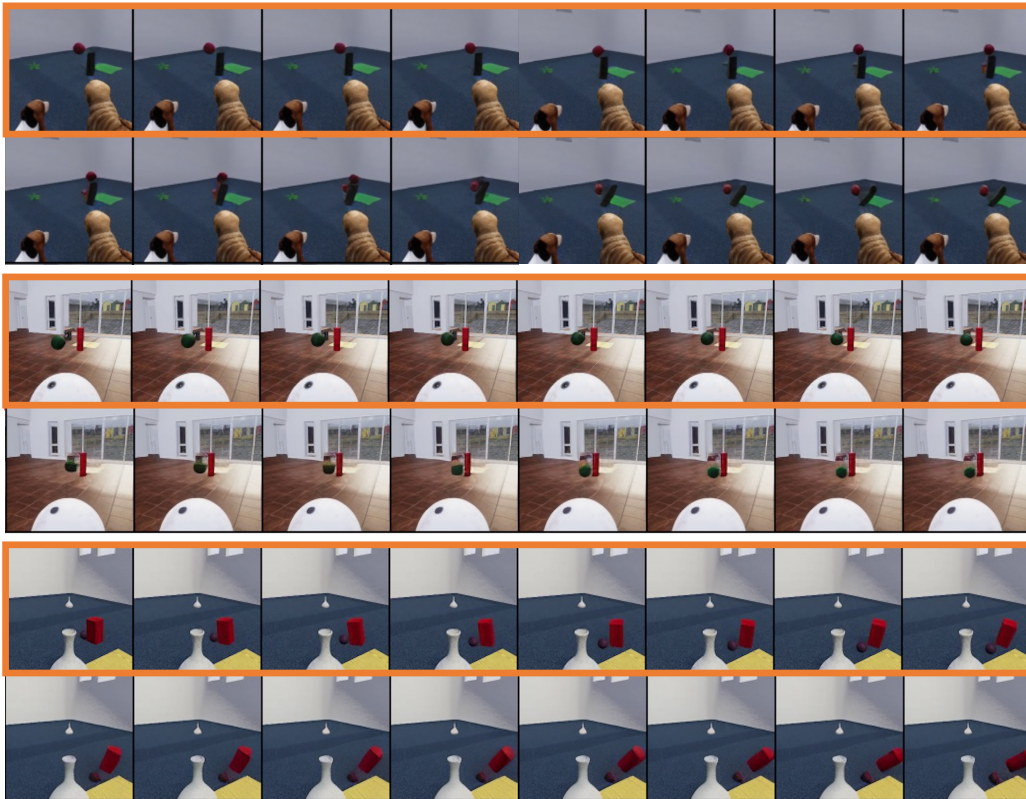


Figure 17: Qualitative video prediction results on the Physion dataset (Bear et al., 2021), where we utilize 8 frames as conditional frames and predict the subsequent 8 frames. In the first example (top two rows) and the third example (bottom two rows), the VDT successfully simulates the physical processes of a ball following a parabolic trajectory and a ball rolling on a flat surface and colliding with a cylinder. In the second example (middle two rows), the VDT captures the velocity/momentum of the ball, as the ball comes to a stop before colliding with the cylinder.

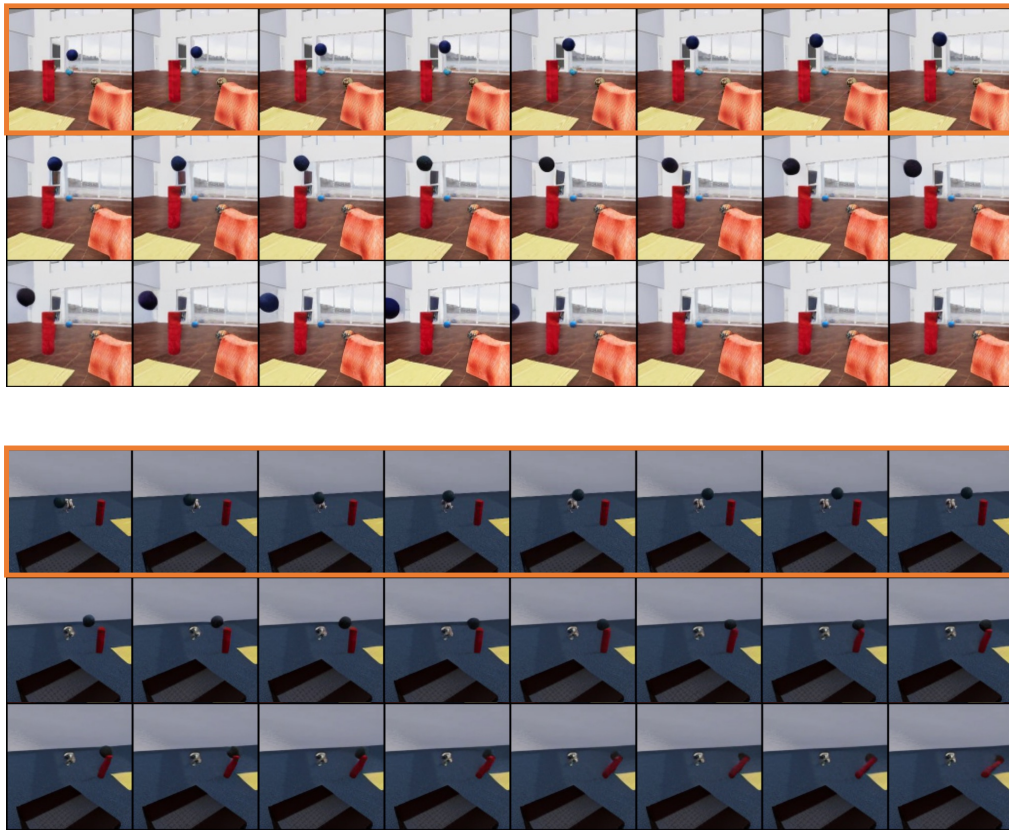
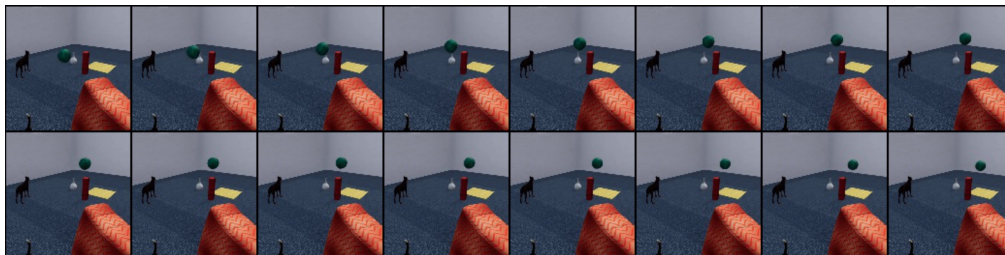
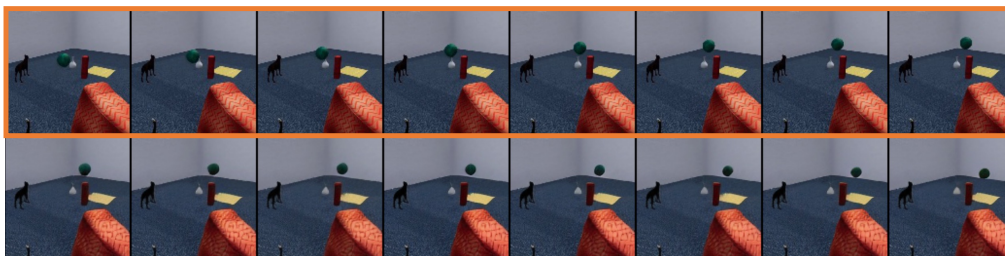


Figure 18: Longer video prediction results (16x128x128) on the Physion dataset (Bear et al., 2021), where we utilize 8 frames as conditional frames and predict the following 8 frames. Subsequently, we predict the next 8 frames based on the previously predicted frames, resulting in a total prediction of 16 frames.

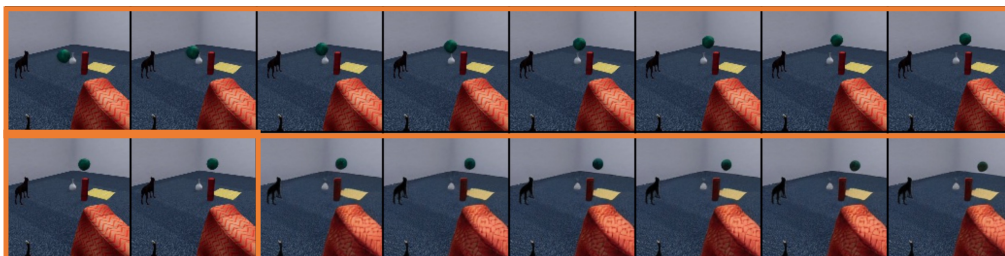
Ground Truth



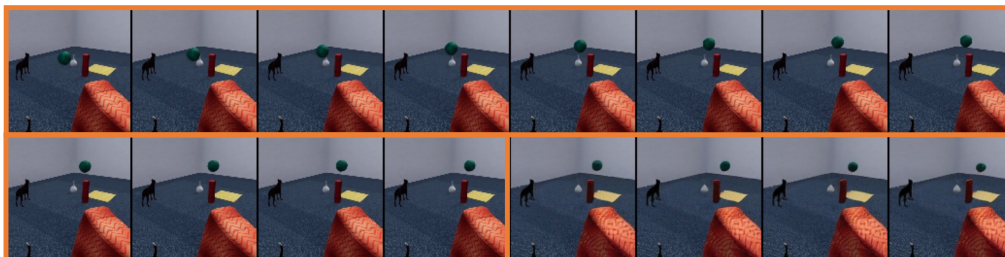
Condition Frame Length: 8 Predict Frame Length: 8



Condition Frame Length: 12 Predict Frame Length: 4



Condition Frame Length: 14 Predict Frame Length: 2



Condition Frame Length: 14 Predict Frame Length: 2

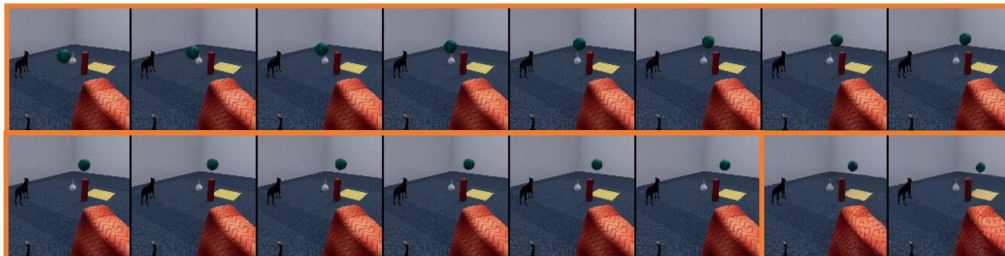


Figure 19: Qualitative video prediction results (16x128x128) on the Physion dataset (Bear et al., 2021). During training, we utilize 8 frames as conditional frames and predict the subsequent 8 frames. Then we zero-shot transfer our VDT to condition frames of different sizes during inference. We observe that our VDT can perfectly generalize to downstream tasks of different lengths without any additional training.

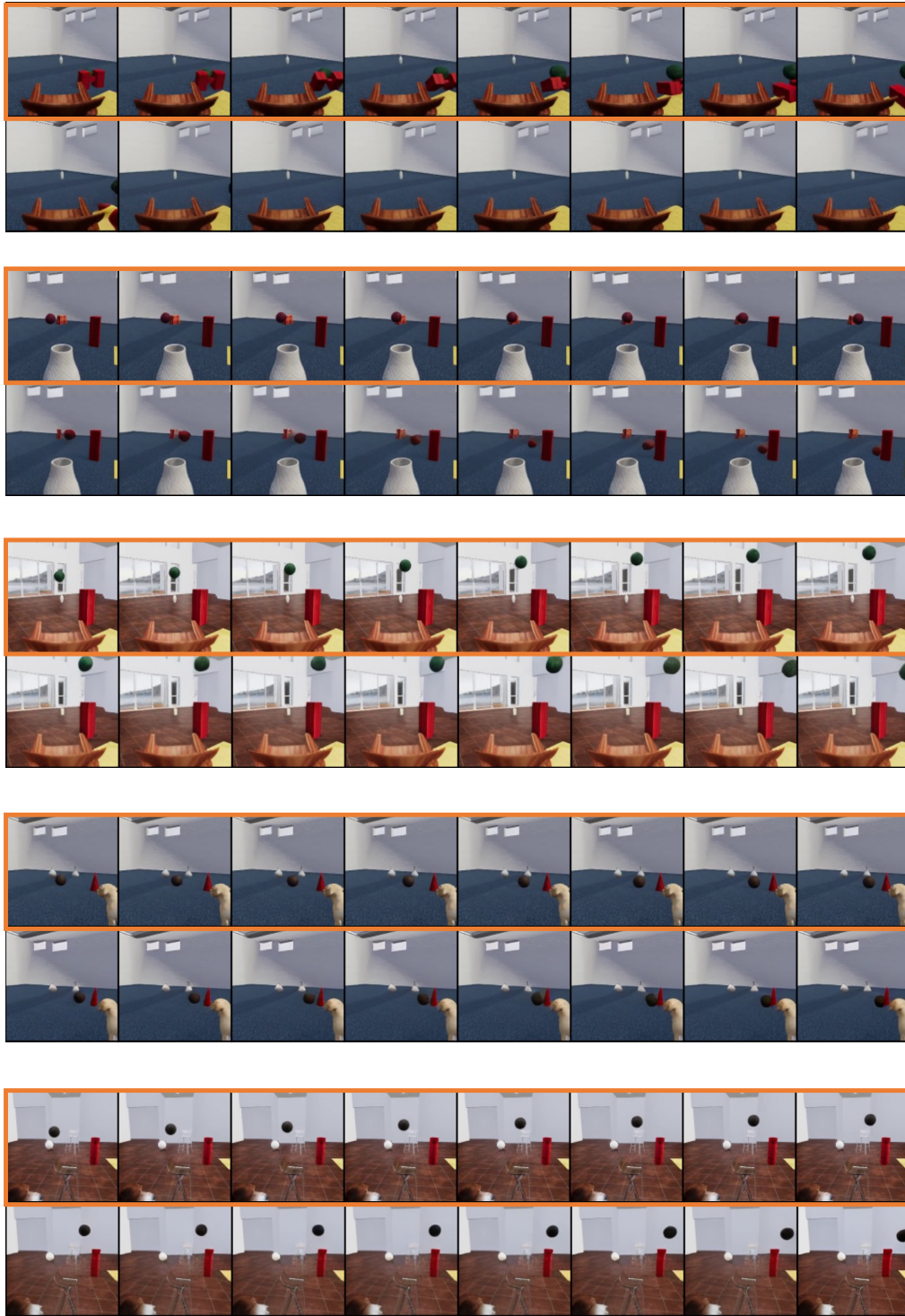


Figure 20: Qualitative video prediction results (16x128x128) on the Physion dataset (Bear et al., 2021), where we utilize 8 frames as conditional frames and predict the subsequent 8 frames.

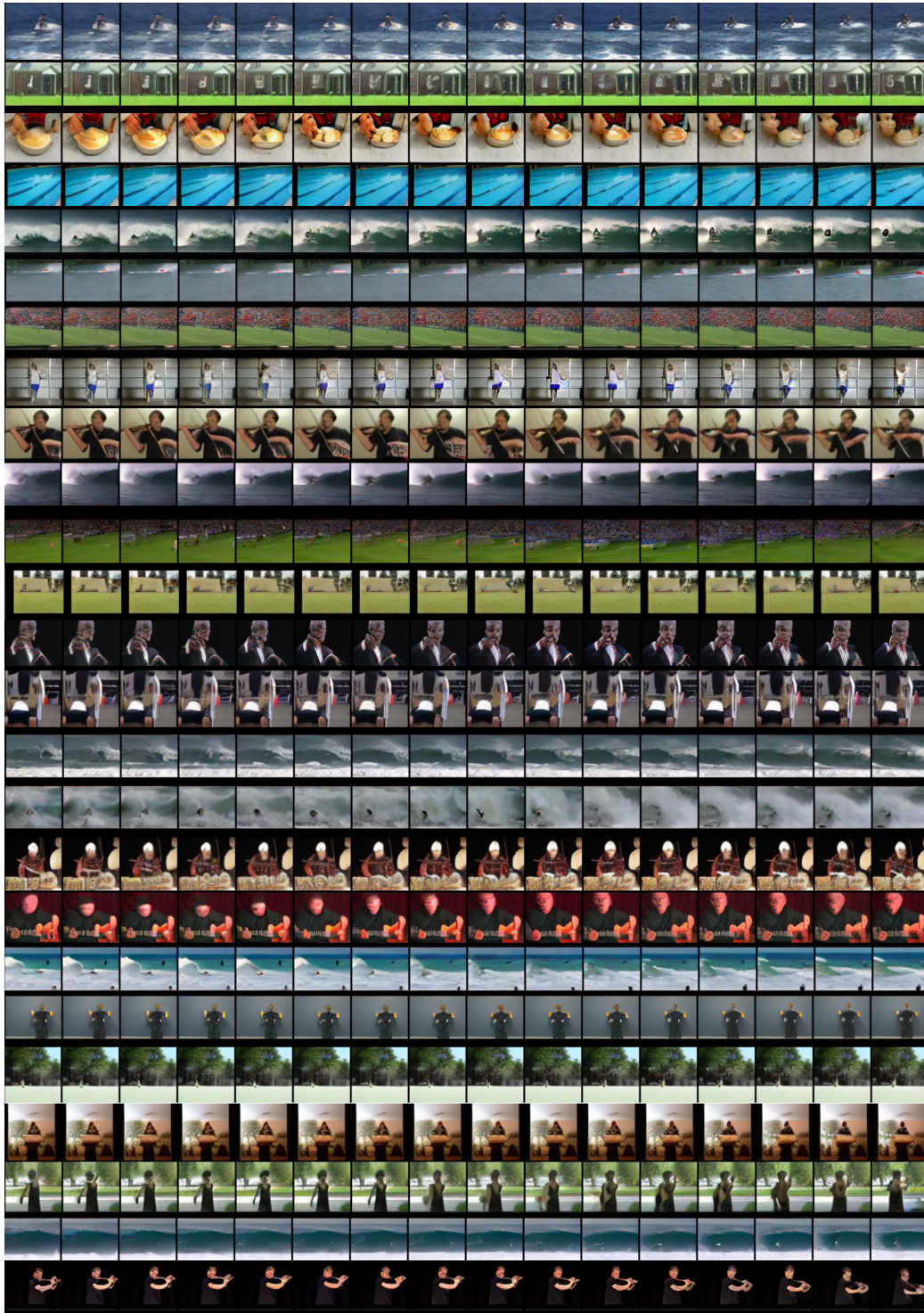


Figure 21: Qualitative unconditional video generation results (16x64x64) on the UCF101 dataset (Soomro et al., 2012).